CMS Physics Analysis Summary

Contact: cms-pag-conveners-susy@cern.ch 2015/08/26

Search for dark matter and compressed mass-spectra supersymmetry with the vector boson fusion topology in proton-proton collisions at $\sqrt{s} = 8$ TeV

The CMS Collaboration

Abstract

The first search for dark matter candidate production through pure electroweak vector boson fusion processes is presented. Events with two jets in the vector boson fusion topology and large missing transverse momentum are analyzed using data from proton-proton collisions at $\sqrt{s} = 8$ TeV collected with the CMS detector. In the context of supersymmetric models with a compressed mass spectrum, which may yield visible particles with momenta too low to detect efficiently, the vector boson fusion topology boosts the momentum imbalance from the escaping lightest supersymmetric particle (a dark matter candidate), providing a distinct signature to discriminate signal events from backgrounds. The dijet mass spectrum measured in data is observed to be compatible with the expected standard model prediction. Limits are set on the production cross section and mass of fermionic dark matter particles in the context of an effective field theory with a heavy mediator, as well as pairs of scalar bottom quarks that are nearly mass degenerate with the lightest supersymmetric particle.

Measurements taken by the Planck satellite indicate 85% of the matter in the universe is composed of dark matter (DM) [1]. The identity of DM is one of the most fundamental open questions in both particle physics and cosmology. Many extensions of the standard model (SM) predict a DM candidate in the form of a weakly-interacting massive particle at the electroweak symmetry breaking scale. R-parity conserving supersymmetric (SUSY) extensions of the SM may naturally contain a DM candidate (a mixture of Bino, Wino, and Higgsino states) as the lightest supersymmetric particle (LSP), which interacts only weakly and is stable [2–6].

Previous LHC SUSY searches have probed DM via prompt decays of heavier particles with signatures which rely on $E_{\mathrm{T}}^{\mathrm{miss}}$, isolated leptons and photons, and/or large p_{T} jets to reduce abundant QCD backgrounds [2–6]. Such search strategies have limited sensitivity in scenarios where the DM mass is close to the mass of the parent, leading to visible particles with too little p_{T} to detect. For example, the ATLAS and CMS bounds on LSP DM from promptly decaying charginos ($\tilde{\chi}^{\pm}$) and neutralinos ($\tilde{\chi}^{0}$), do not surpass the constraints placed by LEP given a mass separation $m_{\pi} \lesssim \Delta m = m_{\tilde{\chi}_1^{\pm}} - m_{\tilde{\chi}_1^{0}} \lesssim 10$ GeV [7, 8]. In the case of long-lived charginos (or neutralinos), a different technique is employed [9, 10].

This paper describes a general search for new physics with missing transverse momentum ($E_{\mathrm{T}}^{\mathrm{miss}}$) and two associated jets using the vector boson fusion (VBF) topology, which is characterized by the presence of two jets with large dijet invariant mass (m_{jj}), in opposite hemispheres, and with large separation in pseudo-rapidity ($|\Delta\eta_{jj}|$) [11, 12]. Focus is placed on pure electroweak direct DM production and compressed-mass-spectrum scenarios where visible particles produced after the decays of heavier SUSY particles are too soft to be identified in the detector or be distinguishable from the SM backgrounds. Thus, the presence of other particles produced in a boosted system, and in association with such decays, is required to provide a distinct signature which discriminates signal events from SM backgrounds with high efficiency. For chargino and neutralino production, the two jets are mostly produced by pure electroweak vector boson fusion processes, while the boost for squark production is provided by two energetic jets from initial state radiation. The VBF topology naturally generates larger $E_{\mathrm{T}}^{\mathrm{miss}}$ since the momentum of the invisible particles must balance the high p_{T} of the scattered partons. Other searches for DM and compressed mass-spectra achieve a boosted system with the selection of one high transverse momentum (p_{T}) jet from initial state radiation [13]. The VBF topology complements other dedicated searches for DM and compressed mass-spectra while additionally offering a scope to determine the couplings of the DM to the SM electroweak bosons, a complementary and significant clue which can help ascertain the connection to cosmological DM.

The analysis is performed using data collected with the CMS detector in proton-proton collisions at a centre of mass energy of $\sqrt{s} = 8$ TeV at the LHC. The data samples correspond to an integrated luminosity of 18.5 fb^{-1}.

The central feature of the CMS apparatus is a superconducting solenoid of 6 m internal diameter, providing a magnetic field of 3.8 T. Within the superconducting solenoid volume are a silicon pixel and strip tracker, a lead tungstate crystal electromagnetic calorimeter (ECAL), and a brass and scintillator hadron calorimeter (HCAL), each composed of a barrel and two endcap sections. Muons are measured in gas-ionization detectors embedded in the steel flux-return yoke outside the solenoid. Extensive forward calorimetry complements the coverage provided by the barrel and endcap detectors. The trigger thresholds in a two-level trigger system are tuned to accept a few hundred data events per second from the proton-proton interactions. A more detailed description of the CMS detector can be found in Ref. [14].

Candidate signal events are recorded with dedicated trigger conditions that require events to

satisfy $E_{\mathrm{T}}^{\mathrm{miss}} > 65$ GeV and contain two jets with $p_{\mathrm{T}} > 35$ GeV in the VBF topology. The jet p_{T}, $\Delta\eta$, and m_{jj} requirements (VBF selection) defining the search region are chosen to achieve a trigger efficiency greater than 98%. We require exactly two jets with $p_{\mathrm{T}} > 50$ GeV and $|\eta| < 5$, and veto events with additional jets with $p_{\mathrm{T}} > 30$ GeV. The rejection of additional jets with $p_{\mathrm{T}} > 30$ GeV will be referred to as the additional jet veto (AJV). The jets are required to be in opposite halves of the detector ($\eta_1 \cdot \eta_2 < 0$), well separated in pseudorapidity ($|\Delta\eta| > 4.2$), and with $m_{jj} > 750$ GeV. These events must satisfy a lepton veto by requiring exactly zero isolated muons, electrons, and tau leptons. Electron and muon candidates are required to satisfy $p_{\mathrm{T}} > 10$ GeV and $|\eta| < 2.5$, while tau candidates must have $p_{\mathrm{T}} > 15$ GeV and $|\eta| < 2.5$. Events are required to have at least 250 GeV of missing transverse momentum. In order to reduce top-quark contamination, events must contain no jets identified as a b-quark jet. The QCD multijet background is further reduced by requiring the absolute value of the azimuthal separation between the sub-leading jet and the $E_{\mathrm{T}}^{\mathrm{miss}}$ vector to satisfy $|\Delta\phi(E_{\mathrm{T}}^{\mathrm{miss}}, j_2)| > 0.5$. A broad enhancement in the tails of the observed dijet invariant mass distribution m_{jj} is used to search for the signal.

The main sources of background are $\mathrm{Z}(\rightarrow \nu\bar{\nu})$ + jets, $\mathrm{W}(\rightarrow l\nu)$ + jets, and a significantly smaller contribution from QCD multijet, $\mathrm{t\bar{t}}$, and diboson production. The $\mathrm{Z}(\rightarrow \nu\bar{\nu})$ + jets background has the same topology as the signal, and is mostly irreducible. Leptons in $\mathrm{W}(\rightarrow l\nu)$ + jets events that fail the veto identification criteria contribute to the $E_{\mathrm{T}}^{\mathrm{miss}}$ in the event, making this process an important background in the search.

The jets and $E_{\mathrm{T}}^{\mathrm{miss}}$ are reconstructed with the Particle Flow (PF) algorithm [15]. Jets are required to pass identification criteria designed to reject particles from pileup interactions and anomalous behavior from the calorimeters. For jets with $p_{\mathrm{T}} > 30$ GeV and $|\eta| < 2.5$ (> 2.5), the identification efficiency is $\approx 99\%$ (95%), while 90–95% (60%) of pileup jets are rejected [16]. Jets originating from the hadronization of bottom quarks are identified using the combined secondary vertex algorithm [17, 18]. For b-quark jets with $p_{\mathrm{T}} > 20$ GeV and $|\eta| < 2.4$, the identification efficiency is $\approx 85\%$ with a $\approx 10\%$ fake rate for light quark and gluon jets [18]. Electrons, muons, and hadronic decays of tau leptons (τ_h) are reconstructed and identified using the tracker, calorimeter, and muon systems. Details of reconstruction and identification can be found in [19–21]. The leptons are required to pass isolation criteria in order to maintain a high signal efficiency for the lepton veto by rejecting misidentified leptons from jets. For electrons and muons, isolation is defined as the sum of the p_{T} of the reconstructed PF charged and neutral particles, within a cone of radius $\Delta R = \sqrt{(\Delta\eta)^2 + (\Delta\phi)^2} = 0.3$ centered around the e/μ track. Isolation for τ_h candidates is imposed by applying a dedicated multi-variate discriminator which combines the surrounding energy deposits with the median energy density flow in the event.

Collision data are compared to samples of Monte-Carlo (MC) simulated events. Samples are generated in the context of two signal models: DM pair production with two jets ($\chi\chi jj$) [22], and pair production of the lightest bottom squark and two associated jets ($\tilde{b}\tilde{b}jj$) in the R-parity conserving Minimal Supersymmetric Standard Model (MSSM) [23]. The signal event samples are generated with MADGRAPH (v5.1.5) [24], applying a requirement of $p_{\mathrm{T}} > 30$ GeV on both partons and a pseudorapidity gap of $|\Delta\eta| > 4.2$. The background event samples with a Higgs boson produced through VBF are generated with POWHEG (v1.0r1380) [25]. The MADGRAPH generator (v5.1.3) is used for DY + jets, W + jets, $\mathrm{t\,\bar{t}}$ + jets, and diboson production. All MC samples make use of the CTEQ6L1 and CTEQ6M parton distribution functions (PDF) [26, 27], except for VBF Higgs boson samples which employ CT10 [28]. The POWHEG and MADGRAPH generators are interfaced with PYTHIA (v6.4.22) [29] for parton shower, fragmentation, hadronization, and decay. The generated background samples are processed with a detailed simulation

of the CMS apparatus using the GEANT4 package (v9.4p03) [30], while the response for signal samples is modeled with the CMS fast simulation program [31]. For the signal acceptance and m_{jj} shapes based on the fast simulation, the differences with respect to the GEANT4-based results are found to be small ($< 5\%$). Corrections are applied to account for the differences. When predicted from simulation, the background yields are normalized to integrated luminosity using next-to-next-leading order (NNLO) cross-sections, while the $\tilde{b}\tilde{b}jj$ and $\chi\chi jj$ signal yields are normalized using next-to-leading order (NLO) and leading order (LO) cross-sections respectively [22, 23]. In all MC samples, multiple interactions are superimposed on the primary collision process and events are reweighted such that the distribution of reconstructed collision vertices matches that in data [16].

The general strategy for the estimation of the background contributions in the signal region (SR) relies on isolating various control regions (CR) with an inverted lepton veto. The CRs are constructed in order to measure the VBF efficiency from data, validate the correct modelling of the m_{jj} shapes and efficiency of the non-VBF cuts (central selection), and optionally determine a correction factor for the efficiency of the central selection. The VBF efficiency is defined as the fraction of events in the CR passing the VBF event selection criteria. For the W/Z + jets backgrounds, the following equation is used to determine their contribution to the SR:

$$N_{\mathrm{SR}}^{\mathrm{BG}} = N_{\mathrm{central}}^{\mathrm{BG}} \cdot SF_{\mathrm{central}}^{\mathrm{BG}} \cdot \epsilon_{\mathrm{VBF}} \tag{1}$$

where $N_{\mathrm{SR}}^{\mathrm{BG}}$ is the predicted background rate in the signal region, $N_{\mathrm{central}}^{\mathrm{BG}}$ the predicted rate in simulation without the VBF selections, $SF_{\mathrm{central}}^{\mathrm{BG}}$ the data-to-simulation correction factor for the central selection as determined from the control samples, and ϵ_{VBF} the VBF efficiency, which is determined directly from data.

Since the production of $\mathrm{Z}(\rightarrow \nu\bar{\nu})$ in association with jets has characteristics that are similar to the production of $\mathrm{Z}(\rightarrow \mu^{+}\mu^{-})$ + jets, the topology of $\mathrm{Z}(\rightarrow \nu\bar{\nu})$ + jets events can be reproduced by treating the pair of muons as a pair of neutrinos. The $\mathrm{Z}(\rightarrow \nu\bar{\nu})$ + jets yield is estimated from data using three control regions in order to factorize correction factors and the level of agreement between data and MC for the lepton and b-jet vetos, the modeling of $E_{\mathrm{T}}^{\mathrm{miss}}$, and the measurement of the VBF efficiency. The first control region (Z_CR1) is obtained by replacing the muon veto with a requirement of exactly two muons, removing the veto for additional leptons and b-jets, removing the $E_{\mathrm{T}}^{\mathrm{miss}}$ requirement, and dropping the VBF selection. The measured data-to-MC correction factor is consistent with unity, validating the modeling of the kinematic and geometric acceptance of leptons by simulation. To determine a correction factor for the efficiency of the additional lepton/b-jet vetos and $E_{\mathrm{T}}^{\mathrm{miss}}$ requirement, a second control sample (Z_CR2) is defined with the same selection as Z_CR1, but requiring $E_{\mathrm{T}}^{\mathrm{miss}} > 250$ GeV and applying the veto on additional leptons and b-jets. In order to model $\mathrm{Z}(\rightarrow \nu\bar{\nu})$, the muons are treated as neutrinos by re-computing the $\vec{E}_{\mathrm{T}}^{\mathrm{miss}}$ after subtracting the $\vec{p}_{\mathrm{T}}^{\,\mu\mu}$. The measured data-to-MC correction factor is $SF_{\mathrm{central}}^{\mathrm{BG}} = 0.95 \pm 0.06$, where the uncertainty is a combination of the statistical uncertainty from data and simulation. The level of contamination ($\sim 4\%$) from other background sources is assigned as a systematic uncertainty on the correction factor. Finally, a third control sample (Z_CR3) is defined by the same selection as Z_CR2, but adding the VBF selection. The VBF efficiency is determined directly from data as the ratio of event yields in CR3 and CR2. Table 1 summarizes the data yields and MC predictions for backgrounds in the control regions.

Similar to the estimate of the Z + jets background, the W + jets rate in the SR is determined using control samples obtained with an inverted muon veto, except requiring exactly one muon in

order to suppress the contribution from Z + jets ($> 91\%$ purity). The measured data-to-MC correction factor is $SF^{\mathrm{BG}}_{\mathrm{central}} = 0.80 \pm 0.042$, where the uncertainty is only statistical.

Since $m_{\mathrm{Z}} - m_{\mathrm{W}} \sim 10$ GeV is small compared to the $E_{\mathrm{T}}^{\mathrm{miss}}$ requirement used to define the SR, the VBF efficiencies for the Z + jets and W + jets backgrounds are similar. This is checked in simulation by comparing the m_{jj} distributions in the SR and validated with data in the CRs. Therefore, the Z and W CRs can be combined for the purpose of measuring the VBF efficiency, ϵ_{VBF}. The VBF efficiency has a measured value of $\epsilon_{\mathrm{VBF}} = 0.008 \pm 0.002$.

The small contribution to the SR from the QCD multijet background is estimated using the fractions of events passing the $E_{\mathrm{T}}^{\mathrm{miss}}$ and AJV requirements. Four QCD multijet dominated CRs are defined with similar selections to the SR, but with the following modifications: (A) failing the $E_{\mathrm{T}}^{\mathrm{miss}}$, AJV, and $|\Delta\phi(E_{\mathrm{T}}^{\mathrm{miss}}, j_2)|$ requirements; (B) passing the $E_{\mathrm{T}}^{\mathrm{miss}}$ requirement, failing the AJV requirement, and failing the $|\Delta\phi(E_{\mathrm{T}}^{\mathrm{miss}}, j_2)|$ requirement; (C) failing the $E_{\mathrm{T}}^{\mathrm{miss}}$ requirement, passing the AJV requirement, and failing the $|\Delta\phi(E_{\mathrm{T}}^{\mathrm{miss}}, j_2)|$ requirement; (D) passing the $E_{\mathrm{T}}^{\mathrm{miss}}$ requirement, passing the AJV requirement, and failing the $|\Delta\phi(E_{\mathrm{T}}^{\mathrm{miss}}, j_2)|$ requirement. The QCD multijet background yields in control regions A, B, and C are estimated from data after subtracting the non-QCD background yields using estimations from simulation. The QCD multijet component in region D is then determined as $N^{\mathrm{D}}_{\mathrm{QCD}} = N^{\mathrm{B}}_{\mathrm{QCD}} \cdot N^{\mathrm{C}}_{\mathrm{QCD}} / N^{\mathrm{A}}_{\mathrm{QCD}}$. Since region D is defined with an inverted $|\Delta\phi(E_{\mathrm{T}}^{\mathrm{miss}}, j_2)|$ requirement, the QCD contribution to the SR is obtained by correcting the prediction in region D by the efficiency of the $|\Delta\phi(E_{\mathrm{T}}^{\mathrm{miss}}, j_2)|$ cut, $N_{\mathrm{QCD}}^{|\Delta\phi(E_{\mathrm{T}}^{\mathrm{miss}}, j_2)|>0.5} / N_{\mathrm{QCD}}^{|\Delta\phi(E_{\mathrm{T}}^{\mathrm{miss}}, j_2)|<0.5}$, which is measured from a $\mathrm{Z}(\rightarrow ll)$ + jets control sample with $E_{\mathrm{T}}^{\mathrm{miss}} > 75$ GeV.

The dominant contributions to the total systematic uncertainty on the Z/W + jets background predictions are from the statistical uncertainties of the data used in the CRs for measuring $SF^{\mathrm{BG}}_{\mathrm{central}}$ (5-6.4%) and ϵ_{VBF} (24.3%). The smaller contributions include the contamination from other backgrounds (2%) in the CRs used to measure ϵ_{VBF}, as well as the uncertainties on $SF^{\mathrm{BG}}_{\mathrm{central}}$ due to lepton and b-jet mis-identification efficiency ($< 1\%$), jet energy resolution ($< 1\%$), jet energy scale (2.5%), and trigger efficiency (5%). Due to the data-to-simulation correction factors for the efficiency of the non-VBF selections, both the signal and background are affected by similar sources of systematic uncertainties: the luminosity measurement (2.6%) [32], lepton and b-jet mis-identification efficiency, jet energy resolution, jet energy scale, and trigger efficiency also contribute to the systematic uncertainty on signal. The dominant uncertainty on signal acceptance is due to the modeling of the ϵ_{VBF} in MADGRAPH. The level of agreement between the predicted and observed ϵ_{VBF} in the Z/W + jets CRs, as well as its uncertainty, is treated as a systematic uncertainty on the ϵ_{VBF} for signal samples. The uncertainty on signal acceptance due to the PDF set included in the simulated samples is evaluated in accordance with the PDF4LHC recommendations by comparing CTEQ6.6L, MRST2006, and NNPDF10 PDF sets with the default PDF set (CTEQ 6L) [26, 33, 34]. The dominant uncertainty that contributes to the signal m_{jj} shape variations include the $E_{\mathrm{T}}^{\mathrm{miss}}$ and jet energy scale uncertainties. The background m_{jj} shape uncertainties are evaluated by comparing the predicted and measured m_{jj} shapes in various Z/W + jets low-$E_{\mathrm{T}}^{\mathrm{miss}}$ sidebands, resulting in uncertainties of 6.8-42.0% depending on m_{jj}.

Figure 1 (left) shows the observed and predicted background m_{jj} spectrum in the SR, while Table 1 shows the predicted background rates and observed number of events. The observed yields in the SR are compatible with the background expectations.

The results are used to constraint the production of new phenomena in the context of two signal models: $\chi\chi jj$ and $\tilde{b}\tilde{b}jj$. The interaction between the DM particle, χ, and the electroweak gauge

Table 1: Predicted and observed rates for the control regions and signal region. The yields are used to calculate correction factors for the *central selections* and VBF selection efficiencies. Statistical uncertainties are cited for both the predicted and observed yields.

Sample	Z_CR1	Z_CR2	Z_CR3	W_CR1	W_CR2	W_CR3	SR
$Z_{\ell\ell}$+Jets	$5.1 \cdot 10^6 \pm 4.6 \cdot 10^3$	675.3 ± 35.2	5.6 ± 2.4	$6.0 \cdot 10^6 \pm 4.0 \cdot 10^3$	12.4 ± 4.4	$0.0^{+1.9}_{-0.0}$	$0.03^{+0.17}_{-0.03}$
W+Jets	99.5 ± 20.9	$0.0^{+2.4}_{-0.0}$	$0.0^{+2.4}_{-0.0}$	$6.7 \cdot 10^7 \pm 4.4 \cdot 10^4$	$1.3 \cdot 10^3 \pm 55$	8.0 ± 4.4	43.6 ± 10.3
$t\bar{t}$	$1.7 \cdot 10^4 \pm 158$	1.6 ± 1.4	$0.0^{+0.7}_{-0.0}$	$4.1 \cdot 10^5 \pm 747$	13.4 ± 4.4	$0.0^{+0.7}_{-0.0}$	$0.0^{+0.7}_{-0.0}$
VV	$1.3 \cdot 10^4 \pm 115$	24.0 ± 4.9	$0.02^{+0.25}_{-0.02}$	$1.0 \cdot 10^5 \pm 331$	22.3 ± 5.0	$0.07^{+0.34}_{-0.07}$	$0.4^{+0.7}_{-0.4}$
$Z_{\nu\bar{\nu}}$+Jets	-	-	-	-	-	-	88.2 ± 9.8
$\Sigma_{\text{MC}}^{weighted}$	$5.2 \cdot 10^6 \pm 4.6 \cdot 10^3$	700.9 ± 35.6	5.6 ± 2.4	$7.3 \cdot 10^7 \pm 4.5 \cdot 10^4$	$1.4 \cdot 10^3 \pm 56$	8.0 ± 4.4	132.3 ± 14.3
Data	$5.1 \cdot 10^6$	666	6	$7.1 \cdot 10^7$	$1.1 \cdot 10^3$	9	118

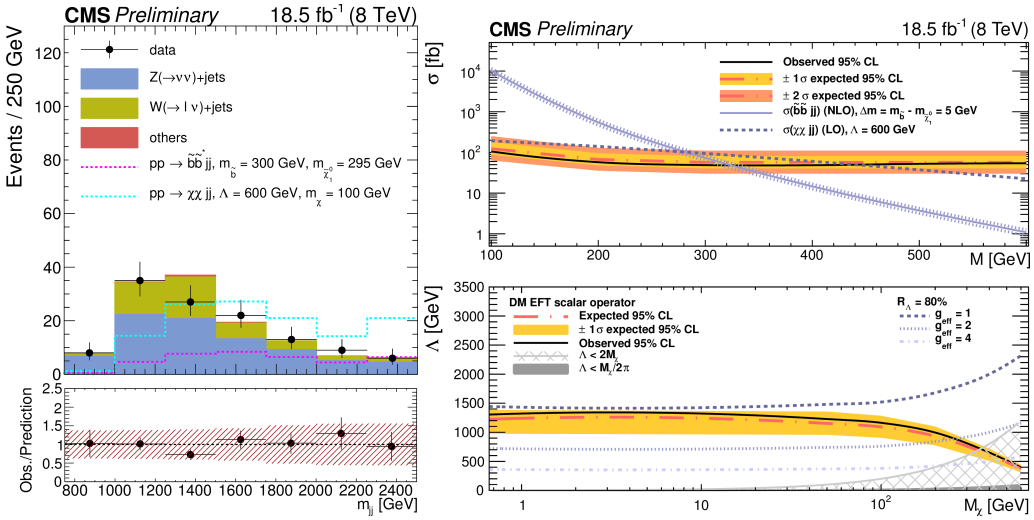

Figure 1: (left) m_{jj} distribution after all signal region selections, where the shaded band in the ratio plot includes the systematic and statistical uncertainties in the background prediction. (upper right) Upper limit at the 95% CL on the cross-section as a function of mass $M = m_\chi = m_{\tilde{b}}$. (lower right) The 95% CL on the contact interaction scale, Λ, as a function of the DM mass, M_χ, for the scalar effective field theory DM model. The validity of the effective field theory is quantified by R_Λ = 80% contours, corresponding to different values of the effective coupling g_{eff}.

bosons of the SM is assumed to be mediated by a heavy particle such that it can be treated as a contact interaction characterized by a scale $\Lambda = \mathcal{M}/g_{eff} = \mathcal{M}/\sqrt{g_\chi g_V}$, where $\mathcal{M}$ is the mass of the mediator, g_χ its coupling to χ, and g_V its coupling to V=γ/Z/W [35]. The DM particle χ is assumed to be a Dirac fermion. In this paper, only the Higgs portal operators of scaling dimension $d = 5$ are considered. For these operators only the 4-point $\chi\chi$VV contact interactions are allowed. In the case of the $\tilde{b}\tilde{b}jj$ signal model, the results are interpreted by assuming $Br(\tilde{b} \to b\tilde{\chi}_1^0) = 1$. The mass difference between $\tilde{b}$ and $\tilde{\chi}_1^0$ is 5 GeV, and thus the $\tilde{b}$ decays into a soft b-quark which is typically not identified. The signal samples were generated for masses of $100 - 600$ GeV, in step sizes of 50 GeV. The signal acceptance for these samples is on the order of 3-6%, depending on the mass.

The calculation of the exclusion limit is obtained by computing the 95% confidence level (CL) upper limit on the signal cross-section using the CL_s method [36, 37]. Systematic uncertainties are represented by nuisance parameters, which are removed by marginalization, assuming a gamma or log-normal prior for normalization parameters, and Gaussian priors for mass-spectrum shape uncertainties.

Figure 1 (upper right) shows the expected and observed upper limits, as well as the theoretical cross-sections, as functions of mass $M = m_\chi = m_{\tilde{b}}$. DM masses below 420 GeV are excluded for a contact interaction scale $\Lambda = 600$ GeV. Since the $\chi\chi jj$ cross-sections are proportional to $1/\Lambda^2$ for contact operators of dimension $d = 5$, results for $\Lambda \neq 600$ GeV can be obtained by appropriately scaling the theoretical cross-section. The validity of the DM signal model using an effective field theory (EFT) approach is quantified by the fraction of signal events, R_Λ, satisfying the condition that the center of mass energy of DM-DM system is less than Λ times g_{eff} of the model. Figure 1 (lower right) shows curves corresponding to R_Λ = 80% with g_{eff} = 1,2,4. The bound is 315 GeV for the compressed mass-spectra scenario of $m_{\tilde{b}} - m_{\tilde{\chi}_1^0} = 5$ GeV, which is determined using the theoretical cross-section minus its one standard deviation uncertainty.

In conclusion, a search has been performed for DM and compressed-mass spectra using events with significant $E_{\mathrm{T}}^{\mathrm{miss}}$ and two jets in a VBF topology. The data corresponds to an integrated luminosity of 18.5 fb^{-1} collected by the CMS detector in proton-proton collisions at $\sqrt{s} = 8$ TeV. It is the first search for pair production of DM particles in pure electroweak processes with couplings to the Z and W bosons of the SM. The observed m_{jj} distribution does not reveal evidence for new physics. Assuming the DM particle is a Dirac fermion, the results are used to exclude a range of masses up to 420 GeV in an effective field theory model with an interaction scale $\Lambda = 600$ GeV and Higgs portal operators of scaling dimension $d = 5$ containing the 4-point $\chi\chi VV$ contact interactions. This analysis also produces the most stringent limits to date on the pair production of $\tilde{b}$ in a compressed-mass spectra scenario defined by mass separation $m_{\tilde{b}} - m_{\tilde{\chi}_1^0} = 5$ GeV, excluding masses below 315 GeV.

Acknowledgements

We congratulate our colleagues in the CERN accelerator departments for the excellent performance of the LHC machine. We thank the technical and administrative staff at CERN and other CMS institutes, and acknowledge support from: FMSR (Austria); FNRS and FWO (Belgium); CNPq, CAPES, FAPERJ, and FAPESP (Brazil); MES (Bulgaria); CERN; CAS, MoST, and NSFC (China); COLCIENCIAS (Colombia); MSES (Croatia); RPF (Cyprus); MoER, SF0690030s09 and ERDF (Estonia); Academy of Finland, MEC, and HIP (Finland); CEA and CNRS/IN2P3 (France); BMBF, DFG, and HGF (Germany); GSRT (Greece); OTKA and NKTH (Hungary); DAE and DST (India); IPM (Iran); SFI (Ireland); INFN (Italy); NRF and WCU (Korea); LAS (Lithuania); CINVESTAV, CONACYT, SEP, and UASLP-FAI (Mexico); MSI (New Zealand); PAEC (Pakistan); MSHE and NSC (Poland); FCT (Portugal); JINR (Armenia, Belarus, Georgia, Ukraine, Uzbekistan); MON, RosAtom, RAS and RFBR (Russia); MSTD (Serbia); MICINN and CPAN (Spain); Swiss Funding Agencies (Switzerland); NSC (Taipei); TUBITAK and TAEK (Turkey); STFC (United Kingdom); DOE and NSF (USA).

Individuals have received support from the Marie-Curie programme and the European Research Council and EPLANET (European Union); the Leventis Foundation; the A. P. Sloan Foundation; the Alexander von Humboldt Foundation; the Belgian Federal Science Policy Office; the Fonds pour la Formation à la Recherche dans l'Industrie et dans l'Agriculture (FRIA-Belgium); the Agentschap voor Innovatie door Wetenschap en Technologie (IWT-Belgium); the Ministry of Education, Youth and Sports (MEYS) of the Czech Republic; the Council of Science and Industrial Research, India; the HOMING PLUS programme of the Foundation for Polish Science, cofinanced from European Union, Regional Development Fund; the Compagnia di San Paolo (Torino); the Consorzio per la Fisica (Trieste); MIUR project 20108T4XTM (Italy); the Thalis and Aristeia programmes cofinanced by EU-ESF and the

Greek NSRF; and the National Priorities Research Program by Qatar National Research Fund.

References

[1] P. Ade et al., "Planck 2013 results. XVI. Cosmological parameters", *Astronomy & Astrophysics* **571** (2014) A16, doi:10.1051/0004-6361/201321591, arXiv:1303.5076.

[2] CMS Collaboration, "Search for new physics in the multijet and missing transverse momentum final state in proton-proton collisions at $\sqrt{s}$= 8 TeV", *JHEP* **06** (2014) 055, doi:10.1007/JHEP06(2014)055, arXiv:1402.4770.

[3] ATLAS Collaboration, "Search for new phenomena in final states with large jet multiplicities and missing transverse momentum at $\sqrt{s}$=8 TeV proton-proton collisions using the ATLAS experiment", *JHEP* **10** (2013) 130, doi:10.1007/JHEP10(2013)130,10.1007/JHEP01(2014)109, arXiv:1308.1841.

[4] CMS Collaboration, "Search for new physics in events with same-sign dileptons and jets in pp collisions at $\sqrt{s} = 8$ TeV", *JHEP* **01** (2014) 163, doi:10.1007/JHEP01(2015)014,10.1007/JHEP01(2014)163, arXiv:1311.6736.

[5] CMS Collaboration, "Search for physics beyond the standard model in events with two leptons, jets, and missing transverse momentum in pp collisions at $\sqrt{s} = 8$ TeV", *JHEP* **04** (2015) 124, doi:10.1007/JHEP04(2015)124, arXiv:1502.06031.

[6] ATLAS Collaboration, "Search for supersymmetry at $\sqrt{s} = 8$ TeV in final states with jets and two same-sign leptons or three leptons with the ATLAS detector", *JHEP* **06** (2014) 035, doi:10.1007/JHEP06(2014)035, arXiv:1404.2500.

[7] CMS Collaboration, "Searches for electroweak production of charginos, neutralinos, and sleptons decaying to leptons and W, Z, and Higgs bosons in pp collisions at 8 TeV", *Eur. Phys. J. C* **74** (2014) 3036, doi:10.1140/epjc/s10052-014-3036-7, arXiv:1405.7570.

[8] ATLAS Collaboration, "Search for direct production of charginos and neutralinos in events with three leptons and missing transverse momentum in $\sqrt{s} = 8$ TeV pp collisions with the ATLAS detector", *JHEP* **04** (2014) 169, doi:10.1007/JHEP04(2014)169, arXiv:1402.7029.

[9] "Constraints on the pMSSM, AMSB model and on other models from the search for long-lived charged particles in proton-proton collisions at $\sqrt{s} = 8$ TeV", *Eur. Phys. J. C* **75** (2015), no. 7, doi:10.1140/epjc/s10052-015-3533-3.

[10] T. C. collaboration, "Search for disappearing tracks in proton-proton collisions at $\sqrt{s} = 8$ TeV", *JHEP* **2015** (2015), no. 1, doi:10.1007/JHEP01(2015)096.

[11] B. Dutta et al., "Vector boson fusion processes as a probe of supersymmetric electroweak sectors at the LHC", *Phys. Rev. D* **87** (2013) 035029, doi:10.1103/PhysRevD.87.035029.

[12] A. G. Delannoy et al., "Probing Dark Matter at the LHC Using Vector Boson Fusion Processes", *Phys. Rev. Lett.* **111** (2013) 061801, doi:10.1103/PhysRevLett.111.061801.

[13] "Searches for third-generation squark production in fully hadronic final states in proton-proton collisions at $\sqrt{s} = 8$ TeV", *JHEP* **2015** (2015), no. 6, doi:10.1007/JHEP06(2015)116.

[14] CMS Collaboration, "The CMS experiment at the CERN LHC", *JINST* **3** (2008) S08004, doi:10.1088/1748-0221/3/08/S08004.

[15] CMS Collaboration, "Commissioning of the Particle-Flow reconstruction in Minimum-Bias and Jet Events from pp Collisions at $\sqrt{s} = 7$ TeV", CMS Physics Analysis Summary CMS-PAS-PFT-10-002, 2010.

[16] CMS Collaboration, "Pileup Jet Identification", CMS Physics Analysis Summary CMS-PAS-JME-13-005, 2013.

[17] CMS Collaboration, "Identification of b-quark jets with the CMS experiment", *JINST* **8** (2013) P04013.

[18] CMS Collaboration, "Performance of b tagging at $\sqrt{s} = 8$ TeV in multijet, ttbar and boosted topology events", CMS Physics Analysis Summary CMS-PAS-BTV-13-001, 2013.

[19] CMS Collaboration, "Performance of electron reconstruction and selection with the CMS detector in proton-proton collisions at vs = 8 TeV", *JINST* **10** (2015) P06005, doi:10.1088/1748-0221/10/06/P06005, arXiv:1502.02701.

[20] CMS Collaboration, "Performance of CMS muon reconstruction in pp collision events at $\sqrt{s} = 7$ TeV", *JINST* **7** (2012) P10002.

[21] CMS Collaboration, "Performance of τ–lepton reconstruction and identification in CMS", *JINST* **5** (2012) P01001, doi:10.1088/1748-0221/7/01/P01001.

[22] W. Beenakker et al., "The Production of charginos / neutralinos and sleptons at hadron colliders", *Phys. Rev. Lett.* **83** (1999) 3780, doi:10.1103/PhysRevLett.100.029901,10.1103/PhysRevLett.83.3780, arXiv:hep-ph/9906298.

[23] W. Beenakker et al., "Stop production at hadron colliders", *Nucl. Phys. B* **515** (1998) 3, doi:10.1016/S0550-3213(98)00014-5, arXiv:hep-ph/9710451.

[24] J. Alwall, "MadGraph/MadEvent v4: The New Web Generation", *JHEP* **09** (2008) 028, doi:10.1088/1126-6708/2007/09/028, arXiv:0706.2334.

[25] S. Frixione, P. Nason, and C. Oleari, "Matching NLO QCD computations with Parton Shower simulations: the POWHEG method", *JHEP* **11** (2007) 070, doi:10.1088/1126-6708/2007/11/070, arXiv:0709.2092.

[26] P. M. Nadolsky et al., "Implications of CTEQ global analysis for collider observables", *Phys. Rev. D* **78** (2008) 013004, doi:10.1103/PhysRevD.78.013004, arXiv:0802.0007.

[27] J. Pumplin et al., "New generation of parton distributions with uncertainties from global QCD analysis", *JHEP* **07** (2002) 012, doi:10.1088/1126-6708/2002/07/012, arXiv:0201195.

[28] H.-L. Lai et al., "New parton distributions for collider physics", *Phys. Rev. D* **82** (2010) 074024, doi:10.1103/PhysRevD.82.074024.

[29] T. Sjöstrand, S. Mrenna, and P. Z. Skands, "PYTHIA 6.4 Physics and Manual", *JHEP* **05** (2006) 026, doi:10.1088/1126-6708/2006/05/026, arXiv:hep-ph/0603175.

[30] GEANT4 Collaboration, "GEANT4: A Simulation toolkit", *Nucl. Instrum. Meth. A* **506** (2003) 250, doi:10.1016/S0168-9002(03)01368-8.

[31] CMS Collaboration, "The fast simulation of the CMS detector at LHC", *J. Phys. Conf. Ser.* **331** (2011) 032049, doi:doi:10.1088/1742-6596/331/3/032049.

[32] CMS Collaboration, "CMS Luminosity Based on Pixel Cluster Counting - Summer 2013 Update", Technical Report CMS-PAS-LUM-13-001, 2013.

[33] A. D. Martin, W. J. Stirling, R. S. Thorne, and G. Watt, "Update of parton distributions atNNLO", *Phys. Lett. B* **652** (2007) 292, doi:10.1016/j.physletb.2007.07.040.

[34] M. Ubiali, "NNPDF1.0 parton set for the LHC", *Nucl. Phys. Proc. Suppl.* **186** (2009) 62, doi:10.1016/j.nuclphysbps.2008.12.020.

[35] R. C. Cotta, J. L. Hewett, M.-P. Le, and T. G. Rizzo, "Bounds on dark matter interactions with electroweak gauge bosons", *Phys. Rev. D* **88** (2013) 116009, doi:10.1103/PhysRevD.88.116009.

[36] A. L. Read, "Presentation of search results: the CL_s technique", *J. Phys. G* **28** (2002) 2693, doi:10.1088/0954-3899/28/10/313.

[37] T. Junk, "Confidence level computation for combining searches with small statistics", *Nucl. Instrum. Meth. A* **434** (1999) 435, doi:10.1016/S0168-9002(99)00498-2.